BNL-105249-2014-TECH

Booster Technical Note No. 205;BNL-105249-2014-IR

ANALYSIS OF SYNCHRONOUS BEAM TRANSFER FROM THE BOOSTER TO THE AGS

S. Y. Zhang

February 1992

Collider Accelerator Department

Brookhaven National Laboratory

U.S. Department of Energy

USDOE Office of Science (SC)

DISCLAIMER

ANALYSIS OF SYNCHRONOUS BEAM TRANSFER FROM THE BOOSTER TO THE AGS

BOOSTER TECHNICAL NOTE
NO. 205

S. Y. ZHANG and W. T. WENG

February 6, 1992

ALTERNATING GRADIENT SYNCHROTRON DEPARTMENT
BROOKHAVEN NATIONAL LABORATORY
UPTON, NEW YORK 11973

ANALYSIS OF SYNCHRONOUS BEAM TRANSFER FROM THE BOOSTER TO THE AGS *

S.Y. Zhang and W.T. Weng

AGS Department, Brookhaven National Laboratory,
Upton, New York 11973

ABSTRACT

In this article, we discuss the physics and component requirements of synchronous beam transfer between the Booster and the AGS, and we also propose a possible scheme for the transfer. After specifying the requirements and tolerances for the transfer, the dynamic models for the frequency pull-in and phase pull-in are presented. Several design problems for the frequency pull-in and the phase pull-in are discussed. Finally, an example is shown and analyzed for a scheme, requiring flatop of both Booster and the AGS, of the synchronous beam transfer from Booster to the AGS.

* Work performed under the auspices of the U.S. Department of Energy

I. Introduction

The Booster circumference is one quarter that of the AGS. During the beam transfer, there are three bunches in the Booster and it takes four transfers to completely fill up the AGS with resultant twelve bunches. The beam transfer from Booster to the AGS requires the entering bunch to match to a designated area and shape of the AGS RF bucket in longitudinal phase space. To preserve the longitudinal emittance, the tolerance of matching in both phase and momentum has to be specified.

If only one transfer is required, the AGS RF system is capable of phase lock onto the incoming three-bunch beam and properly accelerate to full energy without unduly beam blow up or losses. If more than one batch of beam from Booster is to be injected without confusion in the longitudinal plane, a proper frequency and phase lock between the Booster and the AGS, and hence the synchronous transfer, has to happen. These frequency and phase lock is accomplished in two steps. In the first step, the original Booster radial loop as well as the RF frequency reference are disconnected, the AGS RF frequency is used as the reference for a frequency pull-in. In the second step, when the frequency difference is small enough, the system initiates for a phase pull-in. Once the required phase matching is achieved, the beam will be extracted by triggering the fast extraction kicker of the Booster.

In this article, we propose a method for beam transfer with Booster flatop. After specifying the requirements and tolerances, the dynamic models for the frequency pull-in and phase pull-in are presented. Several design problems are discussed, and an example is shown for the beam transfer from Booster to the AGS.

II. Bunch Shape Matching

Useful accelerator and beam parameters of the Booster and the AGS are listed in the following table.

AGS and Booster Parameters at Transfer				
Function	Notation	Booster	AGS	Unit
Harmonic Number	h	3	12	1
Mean Radius of the Accelerator	R	32.114	128.45	m
Magnetic Field	B	0.555	0.0915	$Tesla$
Total Energy of Particle	E	2.473	2.473	GeV
RF Voltage Amplitude	V	48.1	250	KV
RF Frequency	f	4.142	4.142	MHz
RF Angular Frequency	ω_{rf}	26.025	26.025	$Mrad/s$
Transition Energy	γ_t	4.88	8.4	1
Frequency Slip Factor	η	-0.1019	-0.1297	1
Momentum of Particle	p	2.288	2.288	GeV/c
Ratio of Particle Speed to that of Light	β	0.925	0.925	1
$(1-\beta^2)^{-1/2}$	γ	2.636	2.636	1

In the following, the subscripts A and B are used to denote the parameters for the AGS and the Booster, respectively. The Booster magnetic field B_B over acceleration is shown in Fig.1. In this study, the flatop takes about $7ms$, and the beam will be extracted from stationary buckets at the kinetic energy of 1.535 GeV. The corresponding RF voltage program over the same period is shown in Fig.2.

Throughout this paper, δ denotes the largest spread of bucket or bunch variables, such as the phase and momentum spreads, and Δ denotes the displacement of the center of gravity of the bunch variables.

1. Bucket Matching

For stationary bucket, if the RF frequencies are identical for both machines, then

the bucket matching can be satisfied by the bucket height matching requirement alone. The bucket height is related to the momentum spread as follows [1].

$$\frac{\delta p}{p} = (\frac{2eV}{\pi h \beta^2 E \eta})^{1/2} \tag{1}$$

Since at transfer $\beta_B = \beta_A$, and $E_B = E_A$, the matching is satisfied by letting

$$\frac{V_B}{h_B \eta_B} = \frac{V_A}{h_A \eta_A} \tag{2}$$

Thus, for AGS RF voltage amplitude of 250 KV, V_B should be 49.2 KV. This is very close to the predetermined RF voltage program, which needs, therefore, no modification.

We note that the bucket half height at transfer is about

$$W = 2(\frac{eVE\beta^2}{2\pi h \ |\eta| \ \omega_{rf}^2})^{1/2} = 0.56 \ eVs \tag{3}$$

Since the bucket width is $\pm \pi$, the bucket area is 4.48 eVs, which is about 8 times of the bucket half height.

2. Bunch Matching Tolerance

The bunch length of the Booster beam at transfer is about 80 ns, which is equivalent to a bunch width of $\pm$ 1.04 rad. The Booster bunch area is about one third of the bucket area at acceleration, i.e., 0.5 eVs, therefore the bunch half height is $\delta W = 0.153 \ eVs$*.

To first order, the emittance blow-up due to mismatch is given by

$$\frac{\Delta\epsilon}{\epsilon} = \frac{\Delta\phi}{\phi} + \frac{\Delta p}{p} \tag{4}$$

For analysis, we consider the situation of 10 percent error in the phase and 25 percent in the momentum, implying to the emittance blow-up of 35 percent. Then the total

* If the space charge effect is considered, the better strategy is to fill the bucket at acceleration [2], i.e., letting the bunch area equal the bucket area of 1.5 eVs. If in addition the same percentage of the momentum spread is required, then this means a less stringent requirement for the transfer, as shown below.

allowable phase mismatch is

$$\Delta\phi < 1.04\ rad \times 0.1 = 0.104\ rad = 5.9^\circ \tag{5}$$

The tolerance of the momentum displacement can be found through,

$$\frac{\delta p}{p} = \frac{\omega_{rf}}{\beta^2 E}\,\delta W = 0.0123 \times 0.153 = 1.88 \times 10^{-3} \tag{6}$$

Therefore, the total momentum mismatch can be *

$$\frac{\Delta p}{p} < 1.88 \times 10^{-3} \times 0.25 = 4.7 \times 10^{-4} \tag{7}$$

We note that replacing δW in the equation (6) by W in (3), the equivalent momentum displacement corresponding to bucket half height is 6.89×10^{-3}, which is much larger than the allowed transfer error.

3. Momentum Matching

During the transfer, the fluctuation of the magnetic field in both Booster and the AGS would affect the momentum matching. The effect in the AGS can be studied by the following equation [1],

$$\frac{\Delta f_A}{f_A} = \eta_A \frac{\Delta p_A}{p_A} + \gamma_{tA}^{-2}\frac{\Delta B_A}{B_A} = -\,0.1297\frac{\Delta p_A}{p_A} + 0.014\frac{\Delta B_A}{B_A} \tag{8}$$

Before injection, the AGS magnetic field B_A is set at 0.0915 $Tesla$, which gives rise to the ideal RF frequency of 4.142 MHz, same is the Booster RF frequency at the transfer. This frequency can be calculated by the following equation,

$$f_A = \frac{h_A\, c}{2\pi R_A}\,\frac{B_A}{(B_A^2 + (E_0/c\,\rho_A)^2\,)^{1/2}} \tag{9}$$

where E_0 is the rest energy of particle, 0.938 GeV, and ρ_A is the radius of curvature of the magnets, it is 85.37 m.

---

* E. Raka [2] calculated that for the concern of dilution, at AGS a phase mismatch of 3.5 degrees is equivalent to a 2×10^{-4} momentum mismatch. Therefore, from the dilution point of view the requirement of phase mismatch posed in (5) has roughly an equivalent effect to the momentum mismatch posed in (7).

Due to the large time constant of the AGS main magnet, the short term disturbance of the magnetic field is disregarded, and only the long term repeatability is of concern. For this study, the RF frequency deviation of the AGS is assumed to satisfy,

$$\frac{\Delta f_A}{f_A} < 10^{-5} \tag{10}$$

If the AGS magnetic field fluctuation is assumed to be [3]

$$\frac{\Delta B_A}{B_A} < \frac{1}{4 \times 10^3} = 2.5 \times 10^{-4} \tag{11}$$

From equation (8) we have,

$$\frac{\Delta p_A}{p_A} = 7.7\frac{\Delta f_A}{f_A} + 0.1\frac{\Delta B_A}{B_A} < 7.7 \times 10^{-5} + 2.5 \times 10^{-5} = 1.02 \times 10^{-4} \tag{12}$$

where the worst case of the error has been considered. In other words, the injection momentum mismatch at the AGS, due to ΔB_A and Δf_A, is limited within 1.02×10^{-4}, provided the assumptions in equations (10) and (11) are valid.

For total momentum matching, the error in Booster has to be taken into account. Consider

$$\frac{\Delta f_B}{f_B} = \eta_B \frac{\Delta p_B}{p_B} + \gamma_{tB}^{-2}\frac{\Delta B_B}{B_B} = -0.1019\frac{\Delta p_B}{p_B} + 0.043\frac{\Delta B_B}{B_B} \tag{13}$$

The Booster RF frequency is locked by $f_A + \Delta f_A$ shortly before and during the transfer. If the locking accuracy is required to be within 10^{-6}, then from (10) we have

$$\frac{\Delta f_B}{f_B} < 10^{-5} \tag{14}$$

Let [3]

$$\frac{\Delta B_B}{B_B} < 5 \times 10^{-4} \tag{15}$$

Then from (13) we get

$$\frac{\Delta p_B}{p_B} = 9.8\frac{\Delta f_B}{f_B} + 0.42\frac{\Delta B_B}{B_B} < 0.98 \times 10^{-4} + 2.1 \times 10^{-4} = 3.08 \times 10^{-4} \tag{16}$$

The total momentum mismatching in the transfer therefore is limited by

$$\frac{\Delta p}{p} < 1.02 \times 10^{-4} + 3.08 \times 10^{-4} = 4.1 \times 10^{-4} \tag{17}$$

which is within the limit posed in equation (7), therefore the requirements for the RF frequency and the magnetic field deviations in (10), (11), (14), and (15) can be considered as acceptable choices to satisfy momentum matching.

It is interesting to observe that the large momentum error in the Booster, comparing (12) and (16), is partially due to the smaller transition energy in the Booster.

III. Synchronization

In this section, the synchronization of the Booster bunch to the AGS RF bucket will be discussed. The basic operation consists of two steps [4]. The first step is to bring the Booster beam frequency close to AGS RF frequency. In the normal operation, the Booster beam frequency is regulated through the radial feedback by the radial deviation ΔR. Leaving the Booster radial loop on, it may regard the AGS RF reference as a disturbance and therefore to disturb the frequency pull-in. Therefore, the radial loop will be disconnected when the first step of synchronization is initiated. Once the Booster beam frequency is brought close enough to the AGS RF frequency, the second step of phase pull-in can start.

To understand the dynamics in the synchronization, the general beam control model with phase and radial feedbacks will be introduced, then the models for the frequency pull-in and phase pull-in will be presented. Using these models, several problems encountered in the design are analyzed.

1. Beam Control Model

The general beam control model has been introduced and analyzed in [5] and it is reproduced here as shown in Fig.3, where $\Delta\phi$ and $\Delta\omega_b$ are the beam phase and fre-

quency deviations from the synchronous particle, respectively. In the model the Laplace operator s is used. In frequency domain s can be replaced by $j\omega$, while in time domain, it implies a derivative operation with respect to time. a and b are the machine parameters considered to be constant during a short period of time compared with the synchrotron oscillation. They are defined as

$$a = -\frac{\omega_{id}\eta\gamma_t^2}{R} \tag{18}$$

$$b = -\frac{eV\cos\phi_s c}{2\pi\gamma_t^2\beta E} \tag{19}$$

where ω_{id} is the ideal RF frequency, which is determined from the magnetic field using (9), and ϕ_s is the stable phase.

The loop encircling $\frac{1}{s}$, $\frac{b}{s}$, and a represents the fundamental synchrotron oscillation. The loop encircling $\frac{1}{s}$ and G_1 is the phase feedback, where G_1 represents the phase feedback control electronics. The transfer function of the RF frequency synthesizer, power amplifier and RF cavities is assumed to be unity. In general a phase feedback with a constant gain can represent most important functions of the phase feedback, therefore we may simply let $G_1 = k_1$. The loops involved G_2 and G_1 are the radial plus phase feedbacks. For ease of analysis, we also let $G_2 = k_2$.

2. Frequency Pull-In

The model of frequency pull-in is shown in Fig.4, where the original radial feedback is disconnected, instead there is a beam frequency deviation feedback. We note that the Booster beam frequency is

$$\omega_b = \omega_{id} + \Delta\omega_b \tag{20}$$

The AGS RF frequency ω_A in reality is compared with the Booster beam frequency ω_b. It is convenient as shown in Fig.4 that ω_A is compared with ω_{id}, then the error $\Delta\omega_A$ is to drive the small deviation dynamic system. The feedback gain k_2 represents the

feedback network including the frequency to voltage converter.

The purpose of the frequency pull-in is to let the Booster beam frequency ω_b follow the AGS RF frequency ω_A, i.e., to let $\Delta\omega_b$ follow $\Delta\omega_A$. In the tracking, the beam phase deviation $\Delta\phi$ should be within a reasonable limit in order not to cause longitudinal dilution. The useful transfer functions are

$$\Delta\omega_b = \frac{k_1 k_2 \Omega^2}{s^2 + k_1 s + (k_1 k_2 + 1)\Omega^2} \delta\omega_A \tag{21}$$

$$\Delta\phi = \frac{k_1 k_2 s}{s^2 + k_1 s + (k_1 k_2 + 1)\Omega^2} \delta\omega_A \tag{22}$$

where $\Omega^2 = -ab$.

One may notice that the frequency pull-in is simply another version of radial feedback, now the feedback is from the beam frequency deviation, which sometimes is called the frequency feedback. The design and analysis therefore can follow the one for original radial control. At the transfer, $a = 2 \times 10^6$, and $b = -42$, thus the synchrotron oscillation is at 1.459 KHz. A possible design is to let $k_1 = 155 \times 10^3$ and k_2 to be around 5×10^{-5}. Note that this is equivalent to the radial feedback with gain $G_2 = 100$, shown in Fig.3. This combination provides damping ratio varying from 1 to 2.8 during the whole acceleration, with 2.8 at the transfer. If such k_1 and k_2 are used for the original Booster beam control system, it provides a reduction of radial deviation by a factor of 7.7 from that without radial feedback.

In other words, when the frequency pull-in is initiated, the original feedback gains need not be significantly changed. The gain of the frequency to voltage converter, of course, should be chosen to accommodate the frequency feedback. The response of $\Delta\omega_b$ for unit step $\Delta\omega_A$ is shown in Fig.5, where the responses corresponding to three different values of k_2, around 5×10^{-5}, i.e., $k_{21} = 5 \times 10^{-4}$, $k_{22} = 5 \times 10^{-5}$, and $k_{23} = 5 \times 10^{-6}$ are shown for comparison. The residual error of the tracking can be represented as

$$\lim_{t\to\infty} \Delta\omega_b = \frac{k_1 k_2}{k_1 k_2 + 1} \Delta\omega_A \tag{23}$$

From (23), k_{23} gives rise to only 43.5 percent tracking of the reference frequency, which may not be good enough. If the residual error is of the only concern, then k_{21} is the best choice.

The beam phase deviation during the first 0.5 *ms* of the frequency pull-in is shown in Fig.6. If the tolerance of phase deviation is chosen to be about 0.1 *rad*, i.e., 5.7°, then a gain of k_{22} allows only 346 *Hz* of $\Delta\omega_A$, which is too small. With a gain of k_{23}, a 3.2 *KHz* is allowed under the same limitation. Therefore, for a frequency pull-in range of 2 *KHz*, k_2 has to be somewhere between k_{22} and k_{23}.

Since the ideal frequency ω_{id} gradually catches up with the AGS RF frequency ω_A, the reference $\Delta\omega_A = \omega_A - \omega_{id}$ is not a step. Instead it is a step at onset, and then it reduces to zero. Therefore, the real bunch phase deviation is smaller than that shown in Fig.6.

The relation of the frequency pull-in and the phase deviation can be expressed as

$$\Delta\omega_b = -\frac{\Omega^2}{s}\Delta\phi \tag{24}$$

which implies that the frequency variation is simply an integration of the phase deviation. It can be estimated as that for a 1 *rad* phase deviation $\Delta\phi$, the Booster frequency ω_b is pulled-in at a rate of 84×10^6 *rad*/sec.

The initial offset of the beam phase deviation and frequency deviation, when the frequency pull-in is started and the radial feedback is disconnected, can be incorporated in the beam dynamic model as steps of $\Delta\phi_d$ and $\Delta\omega_d$ shown in Fig.4. It is assumed that before the system is switched to the frequency pull-in, the radial control was in a normal condition and the centers of gravity of bunches were not in a strong oscillation. Thus, the effects of these small initial offsets will be disregarded in this study.

3. Phase Pull-In

When the frequency error $\omega_b - \omega_A$ is within the designated range, the frequency pull-in is transferred to phase pull-in. The problem in phase pull-in is more complicated than the frequency pull-in. We will explain the process by looking into the following several subjects.

i) Model and Transfer Functions

The model for phase pull-in is shown in Fig.7, where the integrator $\frac{1}{s}$ in the feedback path represents the phase detector, which compares $\Delta\omega_b$ and $\Delta\omega_A$ to detect the phase error between them. $\Delta\phi_{1d}$ can be used to assign an initial offset of the phase detector for the study, and $\Delta\phi_1$ is the overall output of that phase detector.

The transfer functions from $\Delta\omega_A$ to all interested variables are

$$\Delta\omega_b = \frac{k_1 k_2 \Omega^2}{s^3 + k_1 s^2 + \Omega^2 s + k_1 k_2 \Omega^2} \Delta\omega_A \tag{25}$$

$$\Delta\phi = \frac{k_1 k_2 s}{s^3 + k_1 s^2 + \Omega^2 s + k_1 k_2 \Omega^2} \Delta\omega_A \tag{26}$$

$$\Delta\phi_1 = \frac{s^2 + k_1 s + \Omega^2}{s^3 + k_1 s^2 + \Omega^2 s + k_1 k_2 \Omega^2} \Delta\omega_A \tag{27}$$

ii) Design of Phase Pull-In

Before we choose the value of k_2, the phase feedback gain k_1 has to be determined. Since the system is different from the original one with normal phase and radial feedbacks, the gain may have to be modified for optimal performance.

To start, we consider first the phase feedback. With only the phase feedback the root-loci are shown in Fig.8. Three pairs of closed-loop poles for different values of k_1 are indicated in the plot. For the choice of k_1 being 15×10^2, there is a pair of conjugate closed-loop poles with small negative real parts, which imply a slow and oscillatory response. For k_1 being 155×10^2, the conjugate closed-loop poles are with large

negative real parts, and therefore the response is fast and with a weak oscillation. For k_1 being 5×10^4, the dominant closed-loop pole is again with a small negative real part, which implies a slow response.

Given a chosen k_1, k_2 will determine the closed loop poles of the overall system, which is shown in Fig.9. One may notice that for k_1 being 15×10^2, and 5×10^4, there is no satisfactory choice for k_2 to be taken, since they always generate slow responses, probably also oscillatory. With k_1 being around 155×10^2, an acceptable design can be pursued. One may note that this value of k_1 implies an underdamping during the acceleration with a normal radial feedback. In other words, if a very slow response for the phase pull-in is not desired, the original phase feedback gain has to be reduced.

From the denominator of the transfer function, $s^3 + k_1 s^2 + \Omega^2 s + k_1 k_2 \Omega^2$, the Routh-Hurwitz table is shown as follows [6],

s^3	1	Ω^2
s^2	k_1	$k_1 k_2 \Omega^2$
s	$(1 - k_2)\Omega^2$	
1	$k_1 k_2 \Omega^2$	

To guarantee the stability, the first column of the coefficients must be larger than zero. This requires that,

$$k_2 < 1 \tag{28}$$

It is interesting to note that this condition is not dependent on k_1.

Let $k_1 = 155 \times 10^2$, the closed loop poles are shown in Fig.10 for different values of k_2. The responses are slow, fast, and slow as well as oscillatory for $k_{21} = 0.06$, $k_{22} = 0.125$, and $k_{23} = 0.5$, respectively. It is apparently that k_{22} is a better choice among the three different values. In the following study, however, the responses

for all three different gains of k_2 will be showed for comparison.

For a unit step of $\Delta\omega_A$, the responses of $\Delta\omega_b$ and $\Delta\phi$ are plotted in Figs. 11 and 12. From Fig.11, one may see that $\Delta\omega_b$ settles within a little more than 1 ms with a choice of k_{22}. From Fig.12, we observe that with k_{22} the peak beam phase deviation is about 2×10^{-5} rad. Since this is the response for a unit step $\Delta\omega_A$, therefore if $\Delta\phi$ is limited within 0.1 rad, $\Delta\omega_A$ cannot be larger than 800 Hz.

iii) Lock-in Range

If the lock-in range of the phase loop for phase pull-in is exceeded, then the phase pull-in may be affected. The block diagram of the system for the phase locking to $\Delta\omega_A$ can be simplified as in Fig.13 from Fig.7. To roughly estimate the phase lock-in range, the second order subsystem in Fig.13 can be simplified as k_1 by letting $s = 0$. Now the simplified loop gain is k_1k_2. Therefore, the phase lock-in range can be estimated as k_1k_2 [7]. For example, if we choose $k_1 = 155 \times 10^2$, and $k_2 = 0.125$, then the lock-in range is 1938 rad/sec, i.e., 308 Hz.

Often the phase detector has a linear range of 1 rad at the output. The saturation range is about 1.57 times of the linear range. If the linear range is exceeded, the phase pull-in will be affected. If the saturation range is exceeded, the saw-tooth waveform will appear, and the phase pull-in cannot be properly executed. In Fig.14, the output of the phase detector for phase pull-in is plotted. The steady state level of the phase detector for k_{22} is 0.52×10^{-3} rad, which implies that if the linear range of the phase detector is 1 rad, then a 1922 rad/sec frequency reference $\Delta\omega_A$ will let the output of the phase detector to exceed that range. Note that then k_1k_{22} is 1938 rad/sec, therefore the lock-in range is almost equivalent to the phase detector linear range.

Again, since $\Delta\omega_A$ is not a step, the situation in reality will be better than the ones discussed above.

Once k_1 and k_2 are chosen, the phase lock-in range is fixed. The phase detector linear range however may still be affected by the phase detector initial offset. This problem will be discussed in the following subsection.

iv) Initial Offset of Phase Detector for Phase Pull-in

It can be expected that if the initial offset of the phase detector for phase pull-in is not zero, it will affect the response of the phase detector. This problem along with other effects of the non-zero initial offset can be studied by using the beam dynamic model and transfer functions derived above.

The transfer functions due to the nonzero initial offset of the phase detector for phase pull-in are

$$\Delta\omega_b = \frac{k_1 k_2 \Omega^2 s}{s^3 + k_1 s^2 + \Omega^2 s + k_1 k_2 \Omega^2} \Delta\phi_{1d} \tag{29}$$

$$\Delta\phi = \frac{k_1 k_2 s^2}{s^3 + k_1 s^2 + \Omega^2 s + k_1 k_2 \Omega^2} \Delta\phi_{1d} \tag{30}$$

$$\Delta\phi_1 = \frac{s^3 + k_1 s^2 + \Omega^2 s}{s^3 + k_1 s^2 + \Omega^2 s + k_1 k_2 \Omega^2} \Delta\phi_{1d} \tag{31}$$

The responses are shown in Figs.15, 16, and 17. The response of $\Delta\omega_b$ in Fig.15 shows that it settles within the same period of time as that caused by $\Delta\omega_A$, shown in Fig.11. The combined responses of $\Delta\omega_b$ for a 2×10^3 *rad*/sec of $\Delta\omega_A$ and a 1 *rad* or a -1 *rad* initial offsets, as well as the response with zero initial offset, are shown in Fig.18, which shows that if only the response of $\Delta\omega_b$ is concerned, the initial offset of the phase detector for phase pull-in is not a serious problem. The response of $\Delta\phi$ in Fig.16 shows that for 1 *rad* initial offset on the phase detector for phase pull-in, the maximum bunch phase deviation is less than 0.1 *rad* with k_{22}, which is not very significant. The response of the $\Delta\phi_1$ itself in Fig.17 shows that the bias of the initial offset needs several milli-seconds to settle to zero. Therefore, with $\Delta\omega_A$, the phase detector linear range, even the saturation range, may be exceeded at the presence of a

nonzero initial offset of the phase detector. The combined response of $\Delta\phi_1$ for a 3850 rad/sec $\Delta\omega_A$ and a 1 rad initial offset on the phase detector is shown in Fig.19, where k_2 is assigned to be 0.25. The output of the phase detector in this combined case has reached to about 1.55 rad, much higher than the 1 rad linear range.

One may conclude that a phase zero crossing is needed when the frequency pull-in is transferred to the phase pull-in. If this procedure becomes necessary, the frequency difference between ω_A and ω_b, at the time of phase pull-in, cannot be too small, for otherwise one may have to wait for too long for the phase zero crossing. This frequency difference can therefore be chosen between 500 Hz to 1 KHz, corresponding to the longest waiting time of 2 ms to 1 ms. This determines the initial condition for the beam frequency when the frequency pull-in process is terminated.

v) Initial Condition of the Beam Phase

It is not clear yet what role is played by the initial condition on the beam phase deviation when the phase pull-in is initiated. The relevant transfer functions are

$$\Delta\omega_b = \frac{\Omega^2 s^2}{s^3 + k_1 s^2 + \Omega^2 s + k_1 k_2 \Omega^2} \Delta\phi_d \tag{32}$$

$$\Delta\phi = \frac{s^3}{s^3 + k_1 s^2 + \Omega^2 s + k_1 k_2 \Omega^2} \Delta\phi_d \tag{33}$$

$$\Delta\phi_1 = \frac{\Omega^2 s}{s^3 + k_1 s^2 + \Omega^2 s + k_1 k_2 \Omega^2} \Delta\phi_d \tag{34}$$

The responses are plotted in Figs. 20, 21 and 22. The response of $\Delta\phi_1$ in Fig.22 shows that no matter how the value of k_2 is chosen, the initial offset of the beam phase deviation induces almost the same peak level of the output on the phase detector for phase pull-in. This again may cause the output of the phase detector to exceed the linear, even the saturation, range. Since there is no other means to control the initial offset on the beam phase deviation as phase pull-in is initiated, one has to limit the beam phase deviation all the time.

IV. A Possible Scheme for Synchronous Transfer

In this section, a scheme will be proposed to illustrate the principles discussed above. The Booster RF frequency in the period of time from 64 *ms* to 72.4 *ms* is shown in Fig.23, It is assumed that the AGS RF frequency is the same as the Booster flatop RF frequency, which is 4.141698 *MHz*.

1. Frequency Pull-In

From Fig.23, at 64 *ms* the Booster beam frequency is lower than the AGS RF frequency by about 2 *KHz*. If it is decided that at $\omega_A - \omega_b = 2\pi \times 2 \times 10^3\ rad/sec$ the frequency pull-in is initiated, then at this moment, the Booster radial loop is disconnected and the AGS RF frequency is taken as the reference for the frequency pull-in, as shown in Fig.4.

Combining the considerations presented in the above discussion, we choose $k_1 = 155 \times 10^3$, i.e., unchanged from the original phase feedback, and $k_2 = 2 \times 10^{-5}$, which would induce a less bunch phase deviation than using k_{22}, as shown in Fig.6.

To guarantee that the waiting for the next phase zero crossing will not be too long after the frequency pull-in is terminated, a deliberate frequency offset is needed for the reference ω_A. Here a -1 *KHz* shift can be added to the Booster frequency. The resulting Booster beam frequency program is shown in Fig.24, where the ideal Booster RF frequency is also shown for comparison. At approximately 65 *ms*, the frequency difference between $\Delta\omega_A$ and $\Delta\omega_b$ is about 635 *Hz*, the frequency pull-in can be terminated. The largest deviation of the beam frequency from the ideal frequency during the whole frequency pull-in is less than 300 *Hz*, which is equivalent to a 7×10^{-5} frequency error, implying a 0.9 *mm* radius deviation.

In Fig.25, the corresponding Booster beam phase deviation is shown, and the largest phase deviation is about 5°, which is acceptable.

Another source that causes radius deviation is the Booster magnetic field variation. It can be calculated that $\Delta B_B/B_B = 5 \times 10^{-4}$ gives rise to about 1.1 mm radius deviation. Thus in the worst case the total radius deviation can be about 2 mm. To estimate the corresponding phase deviation, we use the relation of

$$\Delta\phi = s\ \frac{\Delta R}{b} \tag{35}$$

Letting the 2 mm radial deviation to be developed in 1 ms and b is -42, equation (35) shows that the phase deviation is 0.048 rad, i.e., 2.75 °, which is not significant.

2. Phase Pull-In

In Fig.24, at about 65 ms the difference of the Booster beam and the AGS RF frequencies is about 635 Hz. We simply choose this value as the point to start the phase pull-in. One may have to wait for the next phase zero crossing on the phase detector. The flattening Booster beam frequency responses shown in Fig.24 guarantees that the frequency difference will not be too small, and the longest period of time will be about 1.5 ms.

As discussed before, at this moment k_1 should be changed to 155×10^2, while k_2 can be chosen to be 0.1, a little smaller than k_{22}. For a phase detector with a linear range of 1 rad, the frequency reference $\Delta\omega_A$ of 613 Hz can be allowed. Since the total range of the phase detector is 1.57 times higher than the linear range, the total tolerable frequency difference the phase detector can handle without causing saw-tooth waveforms is about 1 KHz under the current condition.

If there is no waiting time for the phase detector zero crossing, the frequency response is shown in Fig.26, where the ideal Booster beam frequency is also shown for comparison. Again the maximal frequency difference is less than 300 Hz, therefore the radial deviation can be tolerated. The phase tracking error from 68.5 ms to 72.5 ms is shown in Fig.27. If the phase mismatch is required to be within 10 °, then the beam should be extracted after 69 ms.

In Fig.28, the beam phase deviation during the phase pull-in is shown. The maximum deviation is less than 3°. In Fig.29, the output of the phase detector for the phase pull-in is shown. The highest output is about 70°, which indicates that the operation safe margin of the phase detector is small under the suggested scenario.

V. Conclusions and Discussions

One method of achieving synchronous beam transfer from the Booster to the AGS has been described and analyzed. It has been shown that in the initial phase of frequency pull-in, the only modification to the original Booster RF control system is to replace Booster radial reference by AGS RF frequency. However, during the phase pull-in, the phase feedback gain k_1 has to be reduced to guarantee a proper damping, and the gain k_2 has to be limited according to (28) to guarantee the stability of the feedback control.

In this scheme, 1 *ms* is required for the frequency pull-in, and 4 *ms* for phase pull-in. Allowing 1.5 *ms* for zero crossing, the total time needed for whole synchronous transfer would be in the order of 6.5 *ms*. This elapse time for transfer has to be kept low to limit filling time for the AGS within 0.4 second.

Another method of achieving synchronous beam transfer is to extract the Booster beam on the fly, without flatop in the Booster. Here the waiting time can be completely eliminated, but with more stringent requirements on the timing, field and momentum control. Detailed analysis of this method will be covered in a future report.

Acknowledgment

The authors would like to thank E. C. Raka and J. M. Brennan for information and helpful discussions.

References

[1] C. Bovet, R. Gouiran, I. Gumowski, and K. H. Reich, *A Selection of Formulae and Data Useful for the Design of A.G. Synchrotron,* CERN/MPS-SI/Int, DL/70/4, 1970.

[2] E. C. Raka, Private Communication.

[3] J. W. Glenn and A. V. Soukas, Private Communication.

[4] J. M. Brennan, Private Communication.

[5] S. Y. Zhang and W. T. Weng, *Error Analysis of Acceleration Control Loops of a Synchrotron,* 5th ICFA Beam Dynamics Workshop, Corpus Christi, Texas, Oct. 1991.

[6] K. Ogata, *Modern Control Engineering,* New York: Prentice Hall, 1970.

[7] S. Y. Zhang and W. T. Weng, *Topics on RF Beam Control of a Synchrotron,* AGS Booster Tech. Note, No. 204, BNL, February, 1992.

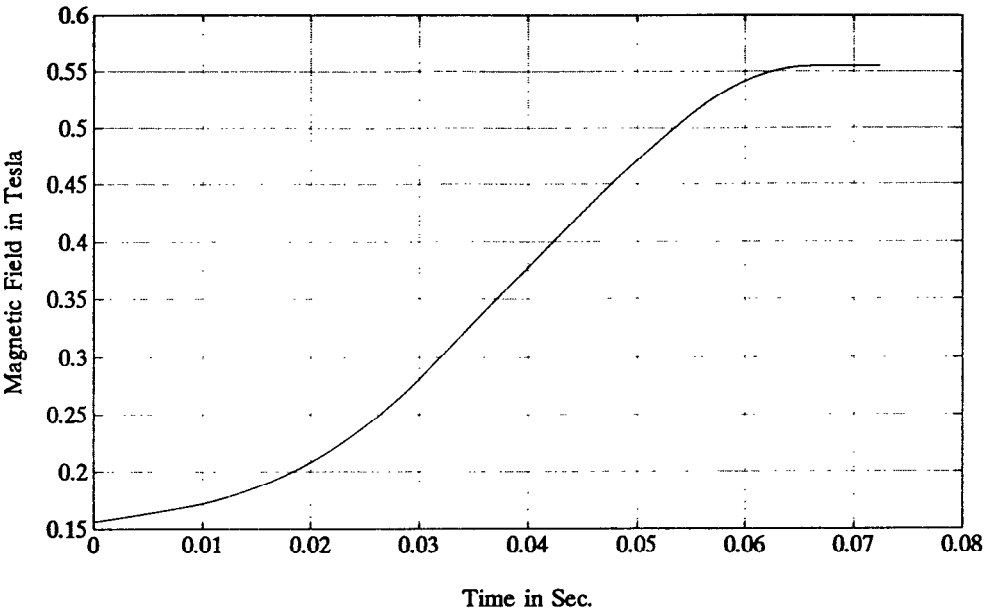

Fig.1. Booster Magnetic Field.

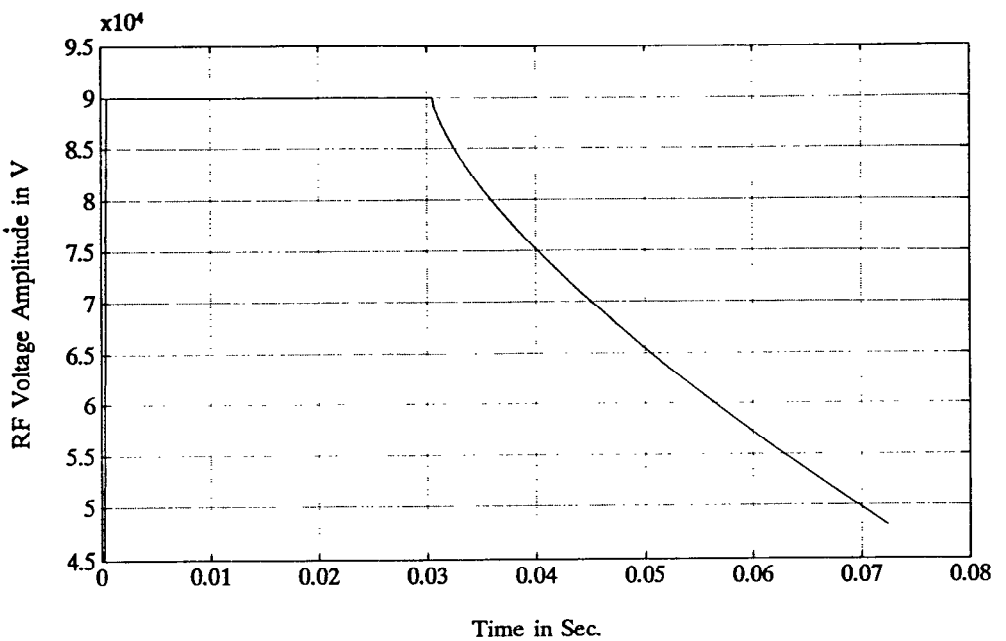

Fig.2. Booster RF Voltage Amplitude Program.

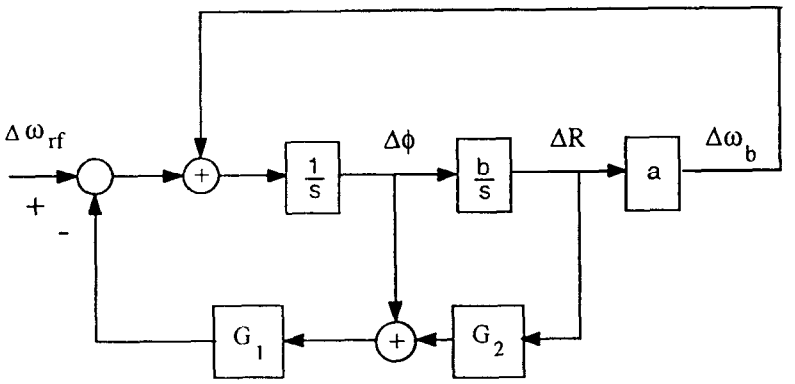

Fig.3. Beam Dynamic Model Under Phase and Radial Feedbacks.

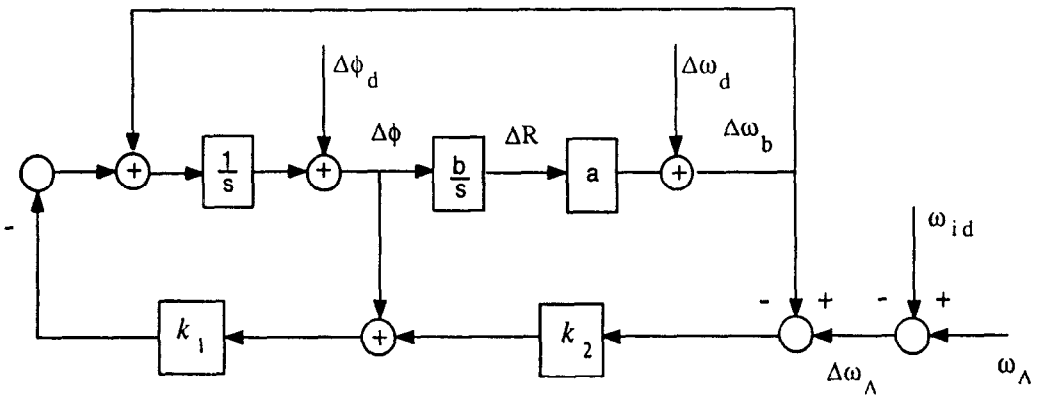

Fig.4. Beam Dynamic Model of Frequency Pull-in.

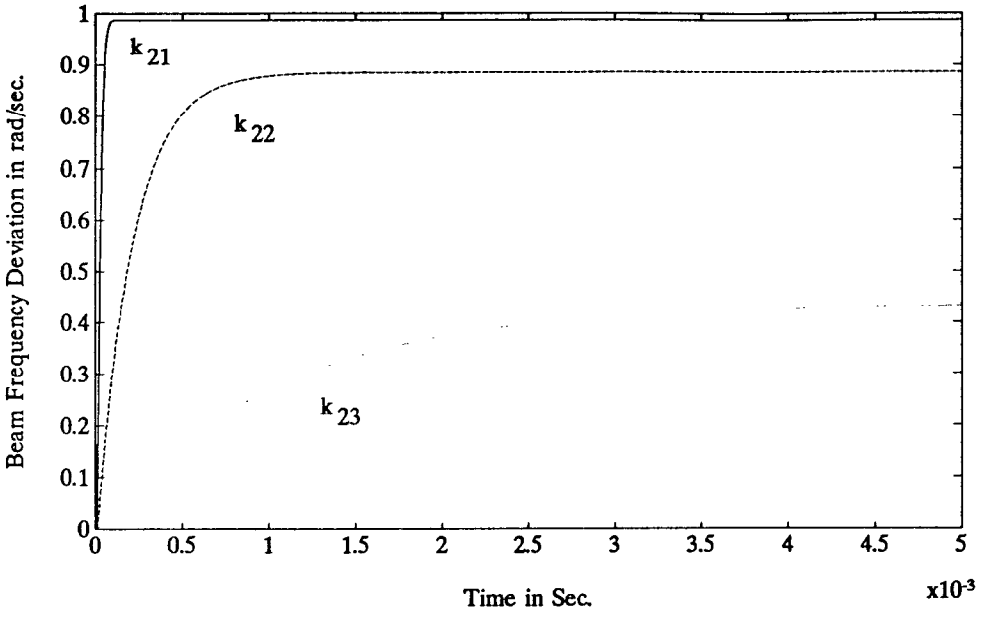

Fig.5. Beam Frequency Deviation due to a Unit Step $\Delta\omega_A$, for Frequency Pull-in.

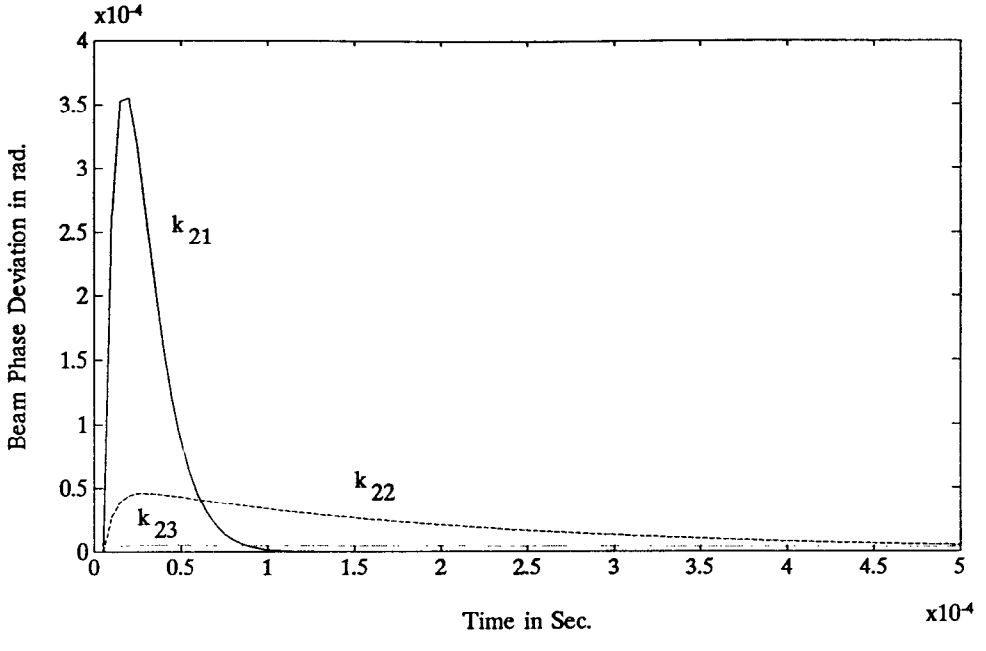

Fig.6. Beam Phase Deviation due to a Unit Step $\Delta\omega_A$, for Frequency Pull-in.

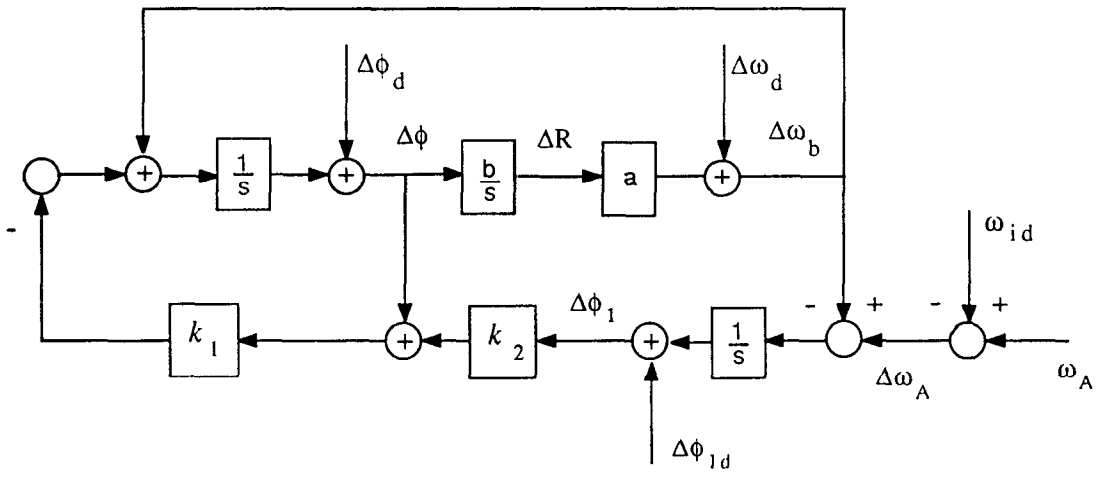

Fig.7. Beam Dynamic Model of Phase Pull-in.

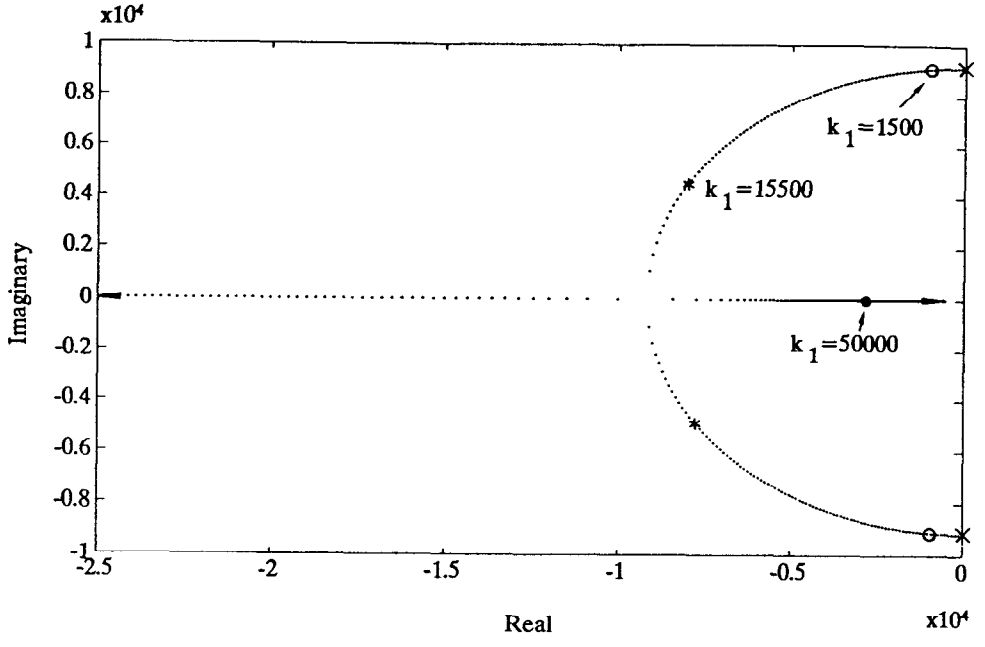

Fig.8. Root Loci of Phase Feedback.

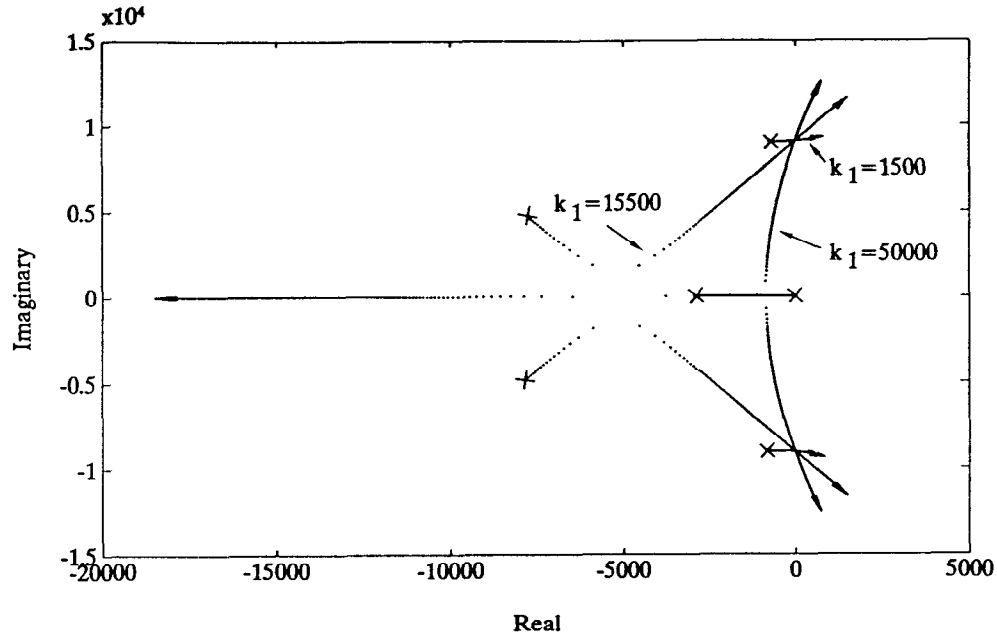

Fig.9. Root Loci of Phase Pull-in, with Different k_1's.

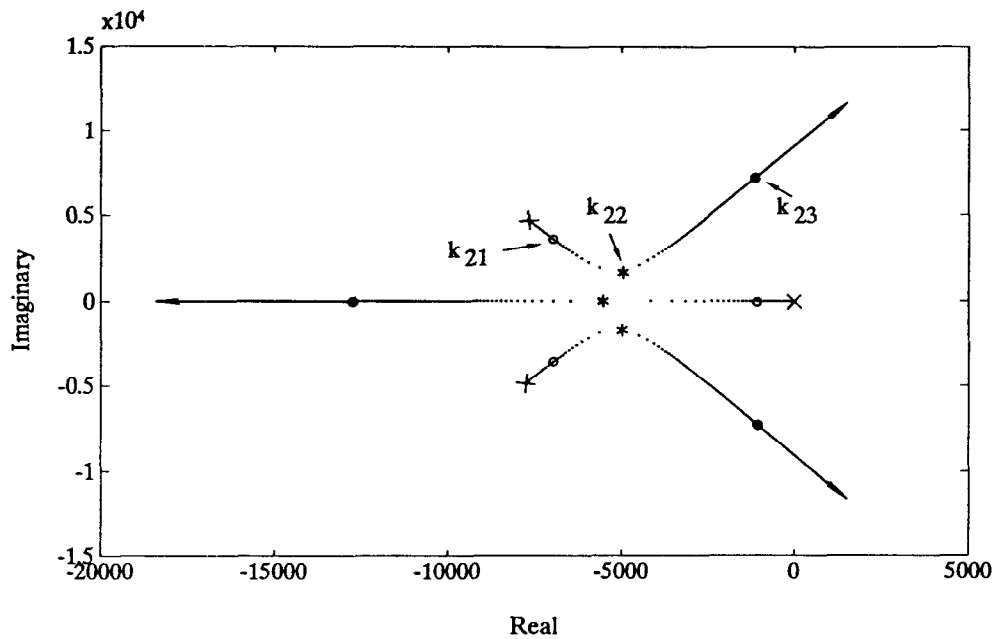

Fig.10. Root Loci of Phase Pull-in, $k_1 = 155 \times 10^2$.

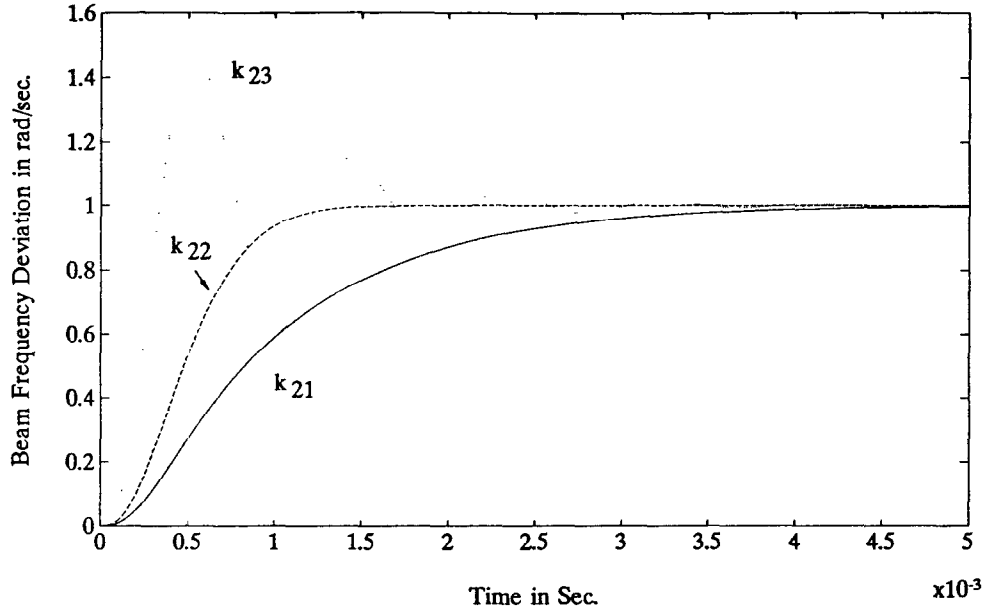

Fig.11. Beam Frequency Deviation due to a Unit Step $\Delta\omega_A$, for Phase Pull-in.

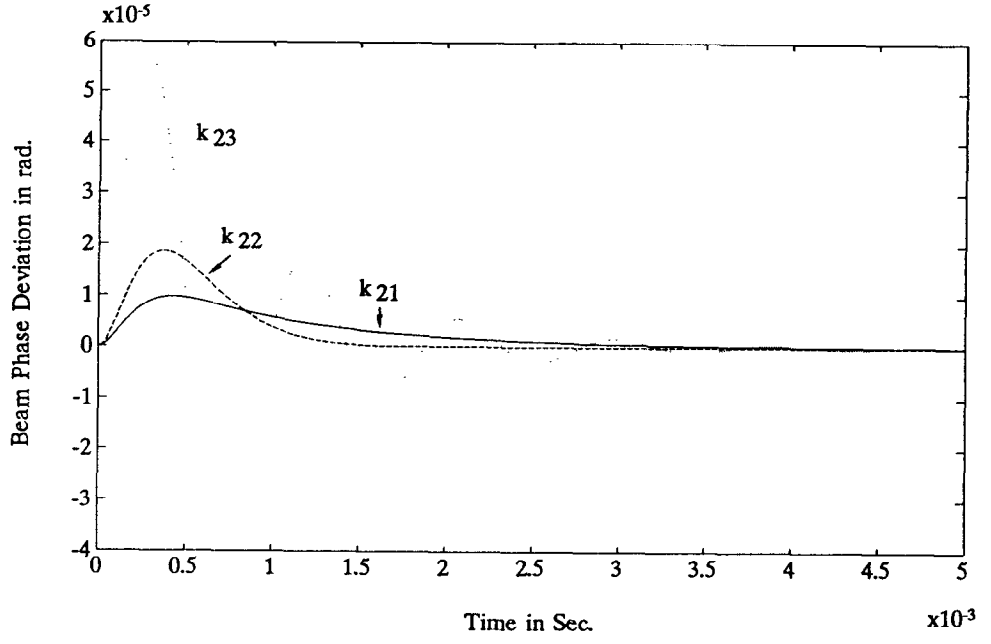

Fig.12. Beam Phase Deviation due to a Unit Step $\Delta\omega_A$, for Phase Pull-in.

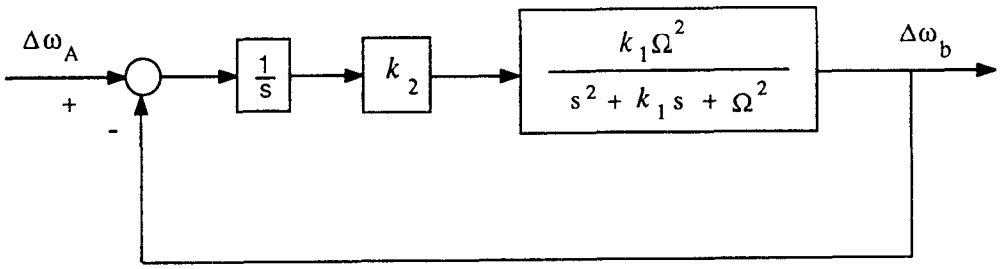

Fig.13. Simplified Dynamic Model for Phase Locking.

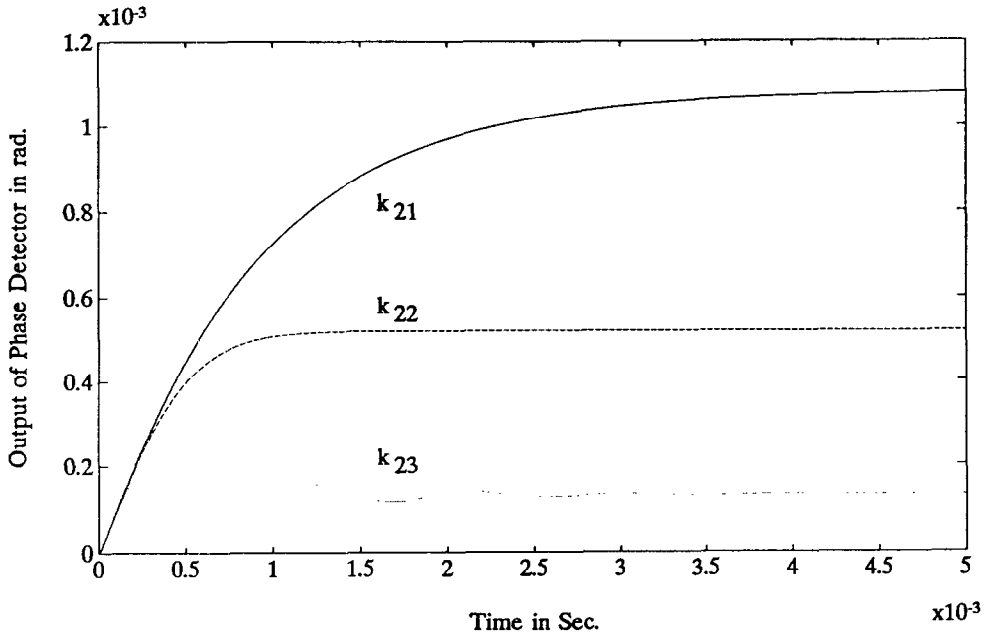

Fig.14. Output of the Phase Detector due to a Unit Step $\Delta\omega_A$.

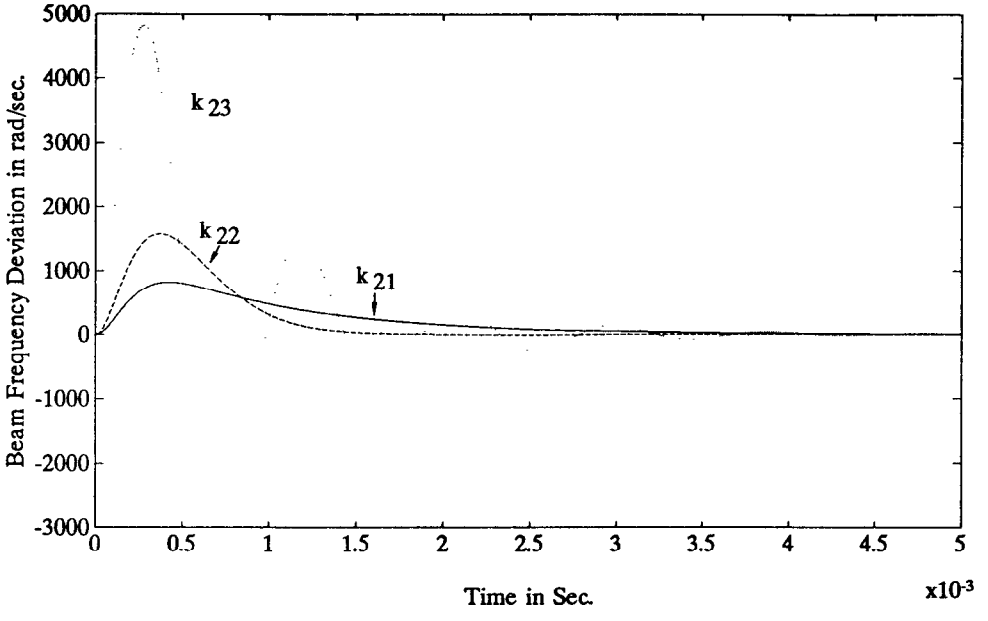

Fig.15. Beam Frequency Deviation due to 1 rad of Initial Offset of $\Delta\phi_{1d}$.

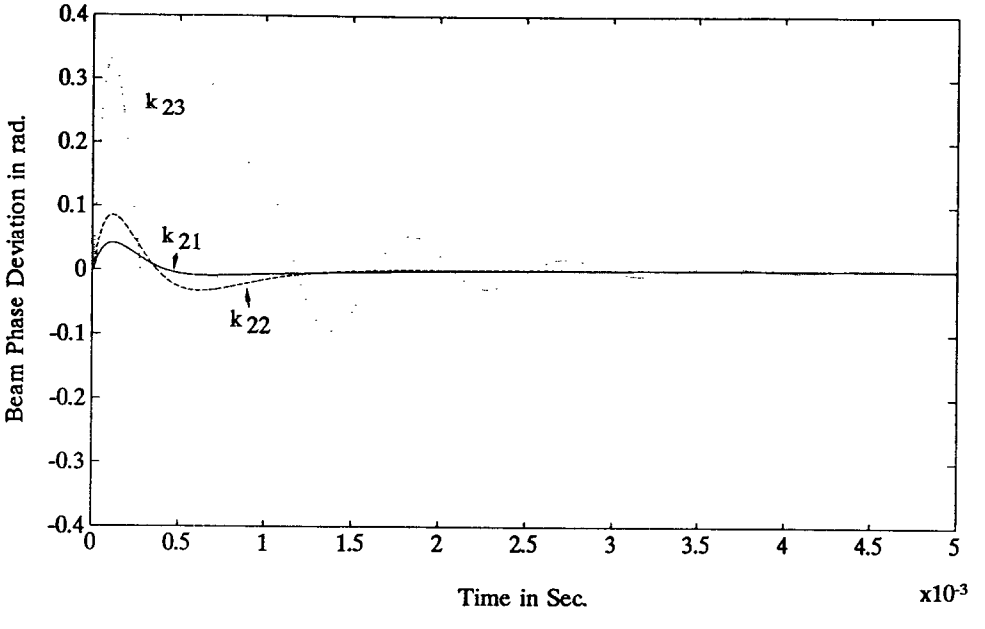

Fig.16. Beam Phase Deviation due to 1 rad of Initial Offset of $\Delta\phi_{1d}$.

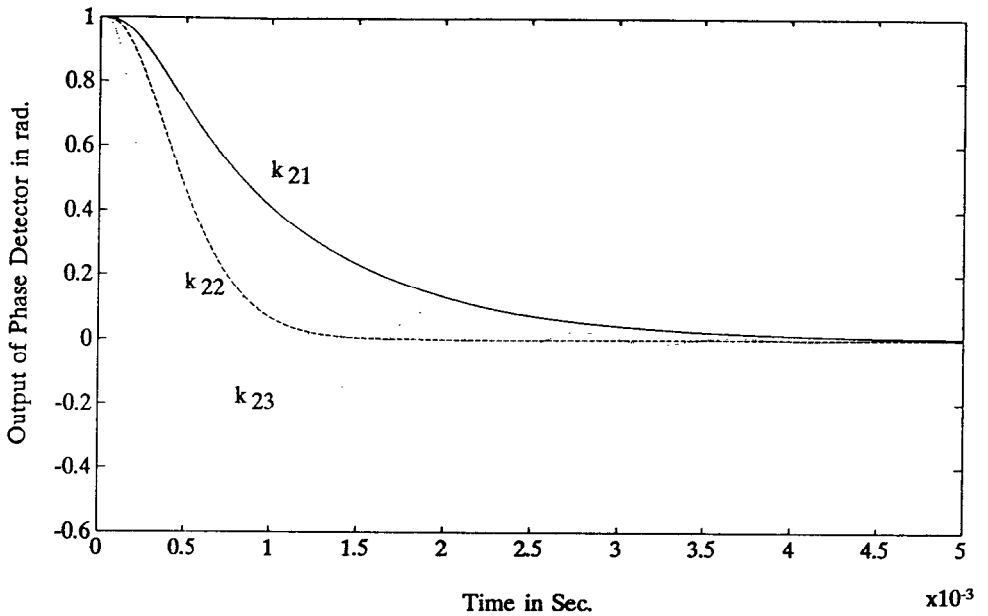

Fig.17. Output of the Phase Detector due to 1 rad of Initial Offset of $\Delta\phi_{1d}$.

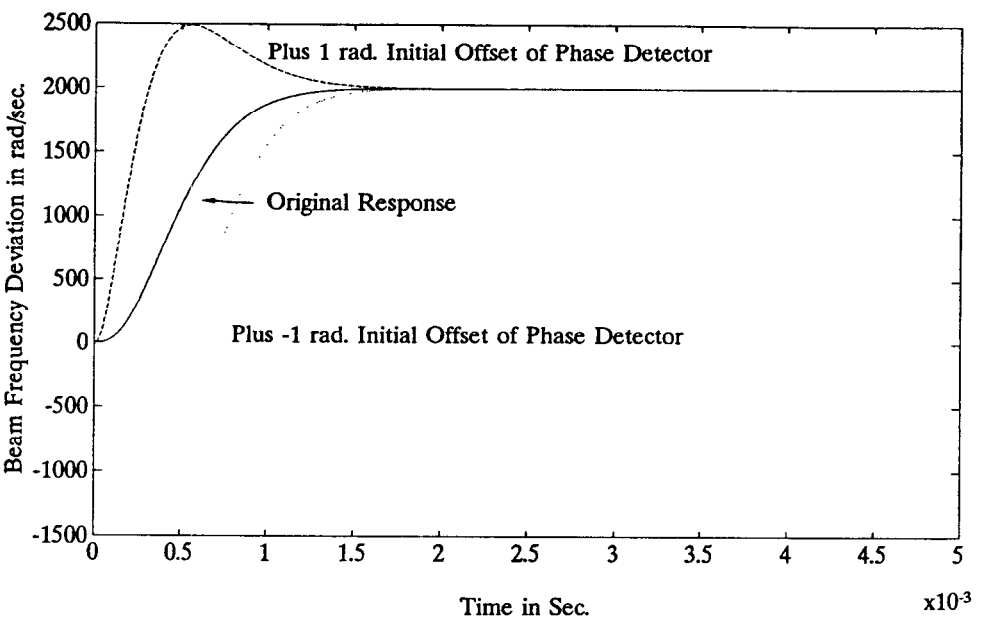

Fig.18. Beam Frequency Deviation due to a Unit Step $\Delta\omega_A$, for Different Initial Offsets of the Phase Detector.

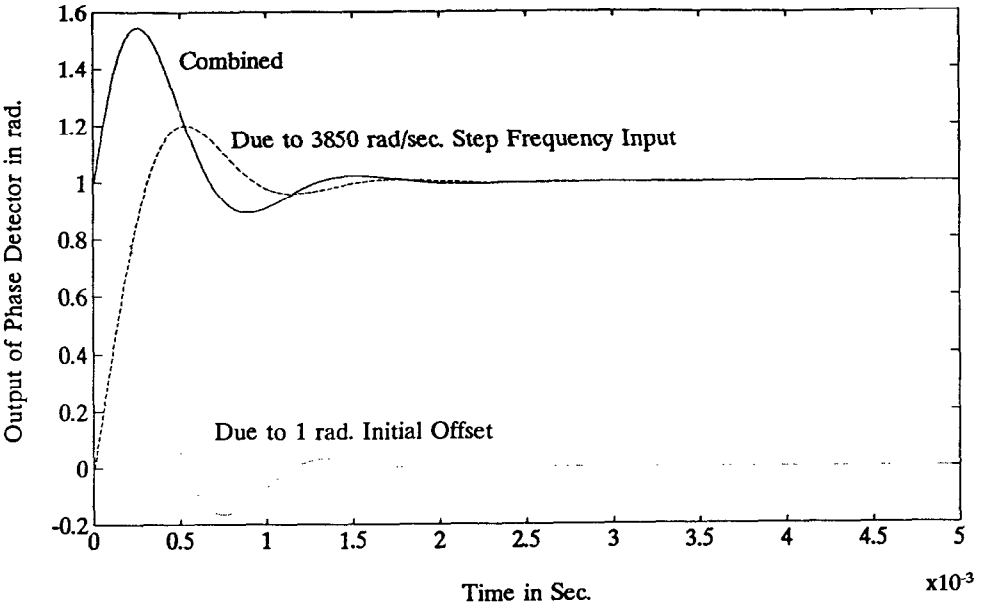

Fig.19. Output of the Phase Detector due to $\Delta\omega_A$, Initial Offset of the Phase Detector, and the Combined.

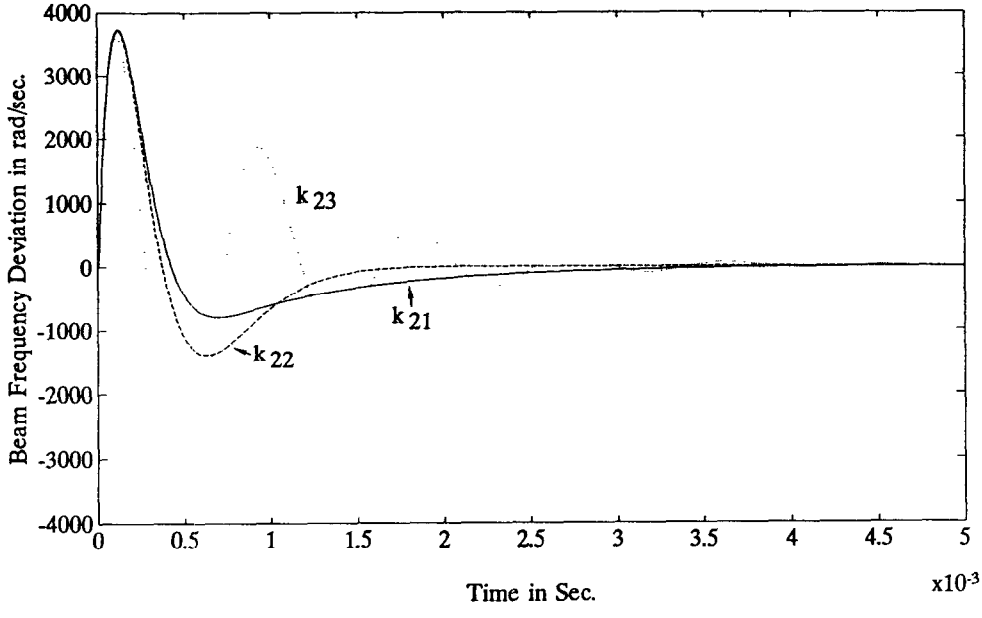

Fig.20. Beam Frequency Deviation due to 1 rad Initial Beam Phase Deviation.

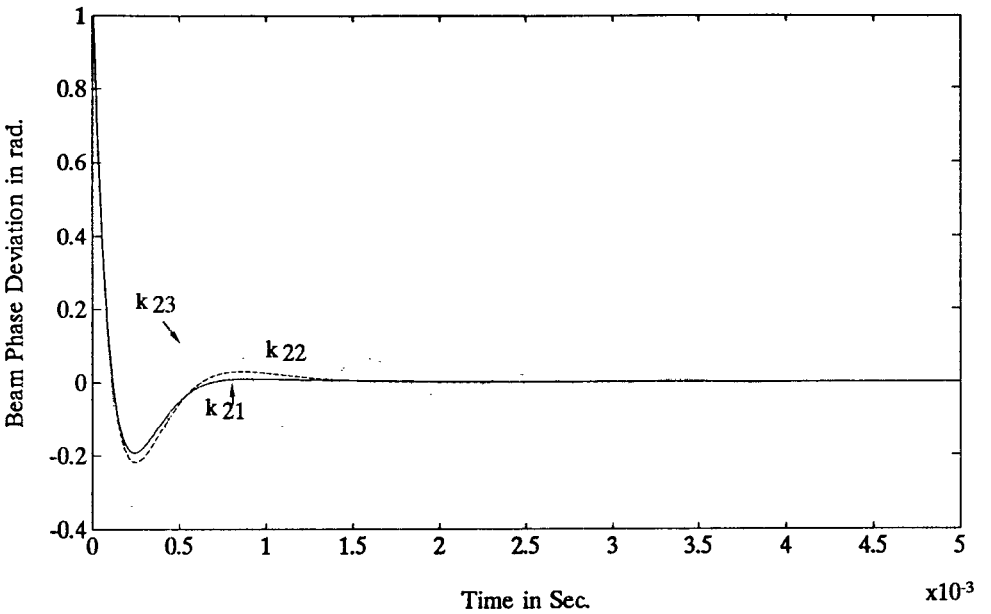

Fig.21. Beam Phase Deviation due to 1 rad Initial Beam Phase Deviation.

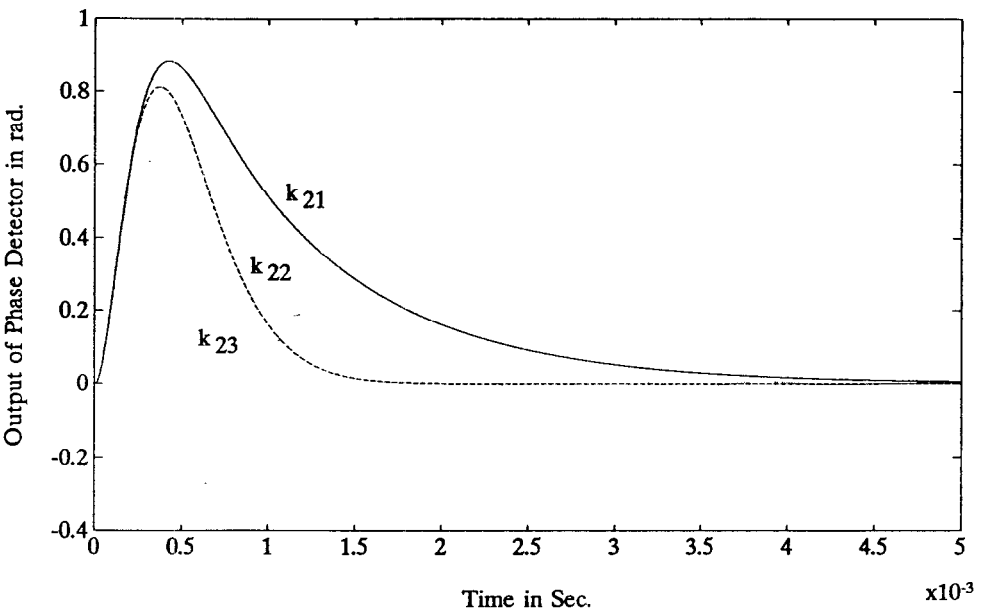

Fig.22. Output of the Phase Detector $\Delta\phi_1$, due to 1 rad Initial Beam Phase Deviation.

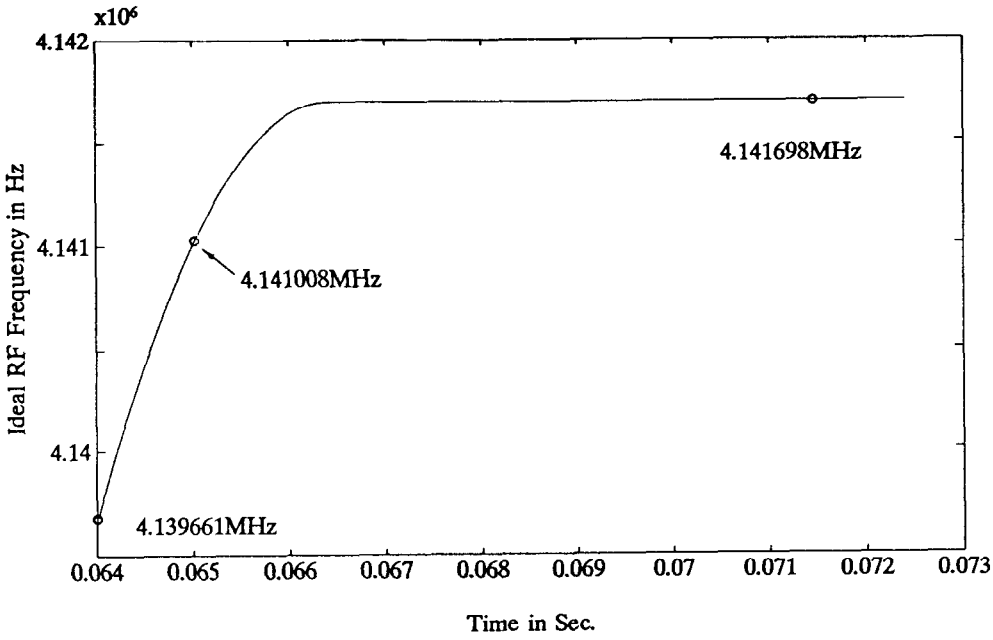

Fig.23. Booster Ideal RF Frequency, from 64 ms to 72.4 ms.

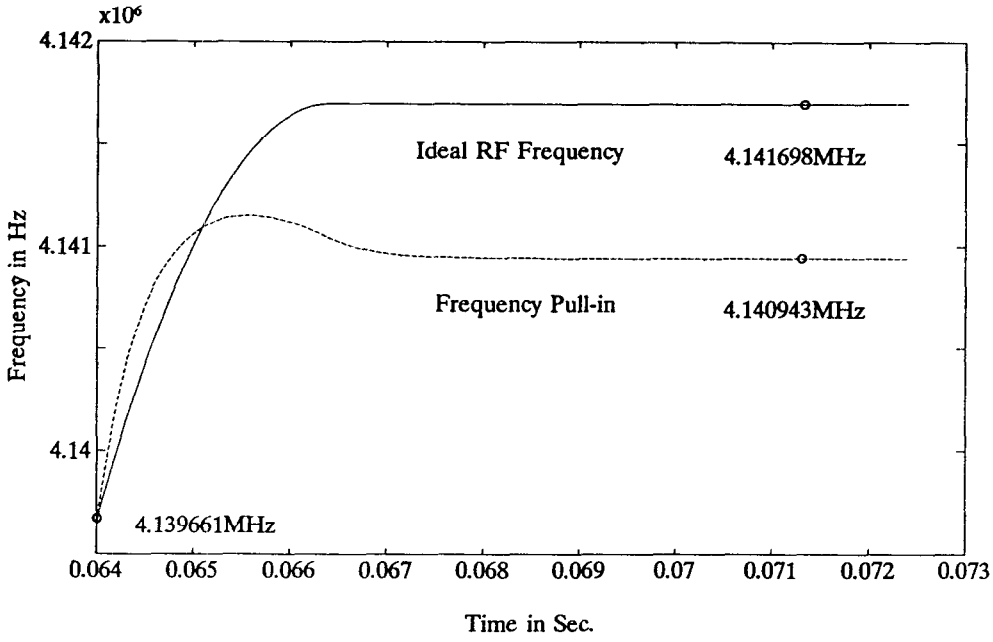

Fig.24. Beam Frequency with Frequency Pull-in, and the Booster Ideal RF Frequency.

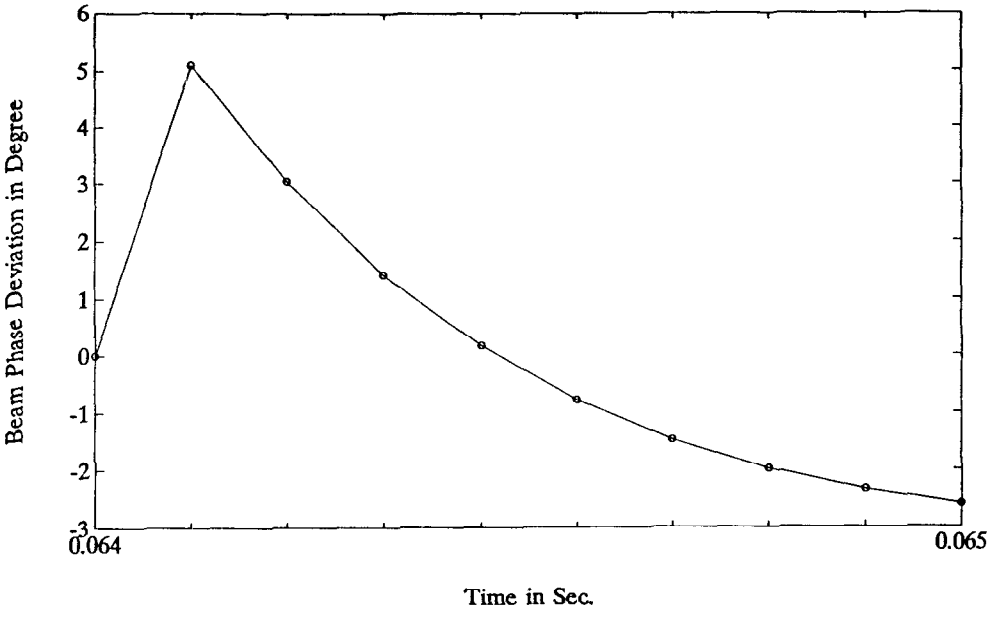

Fig.25. Beam Phase Deviation during Frequency Pull-in.

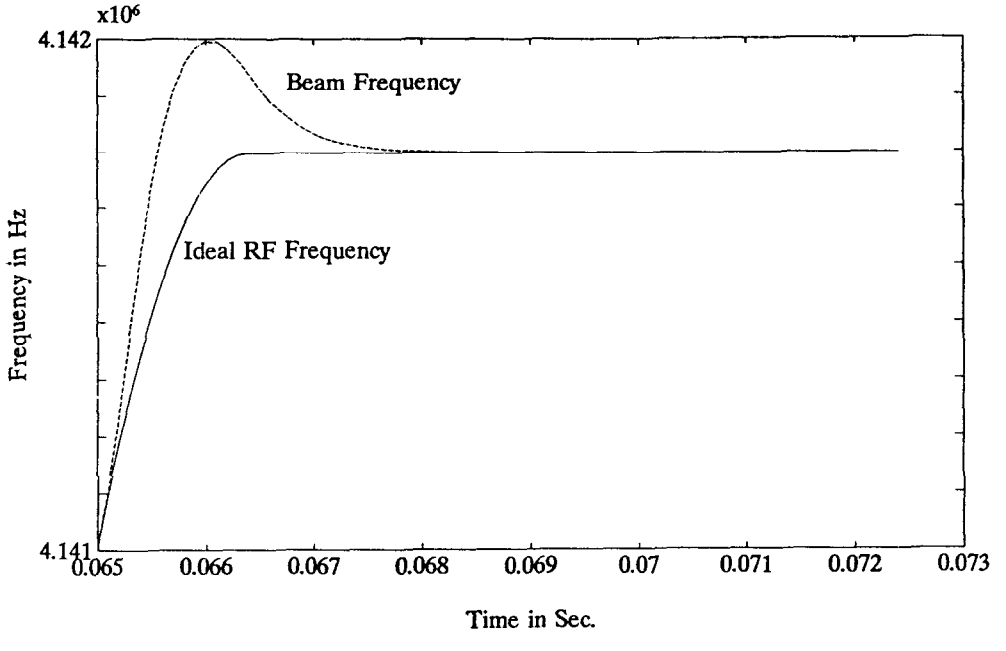

Fig.26. Beam Frequency during Phase Pull-in.

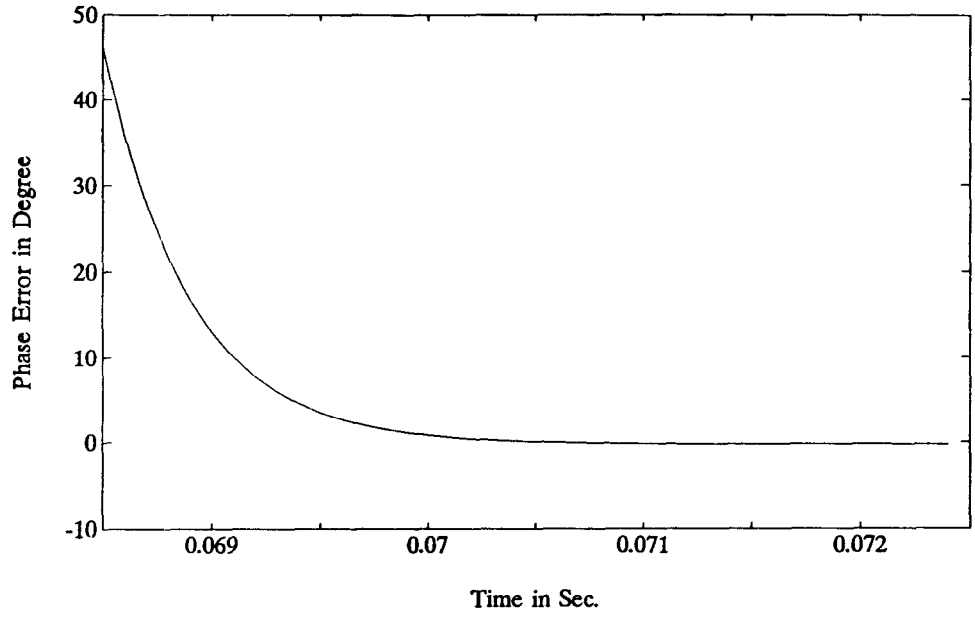

Fig.27. Phase Tracking Error from 68.5 *ms* to 72.5 *ms* during Phase Pull-in.

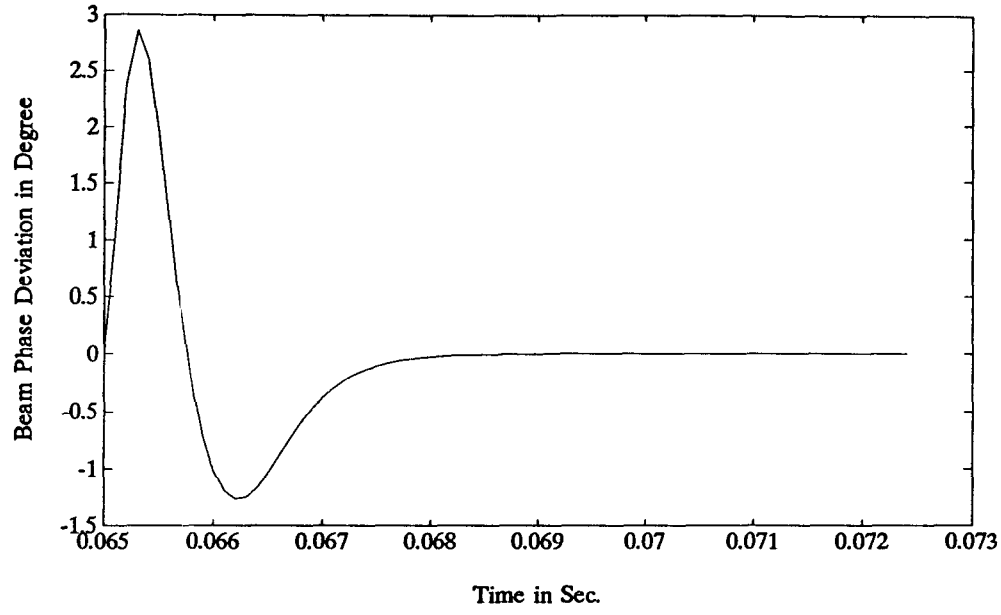

Fig.28. Beam Phase Deviation during Phase Pull-in.

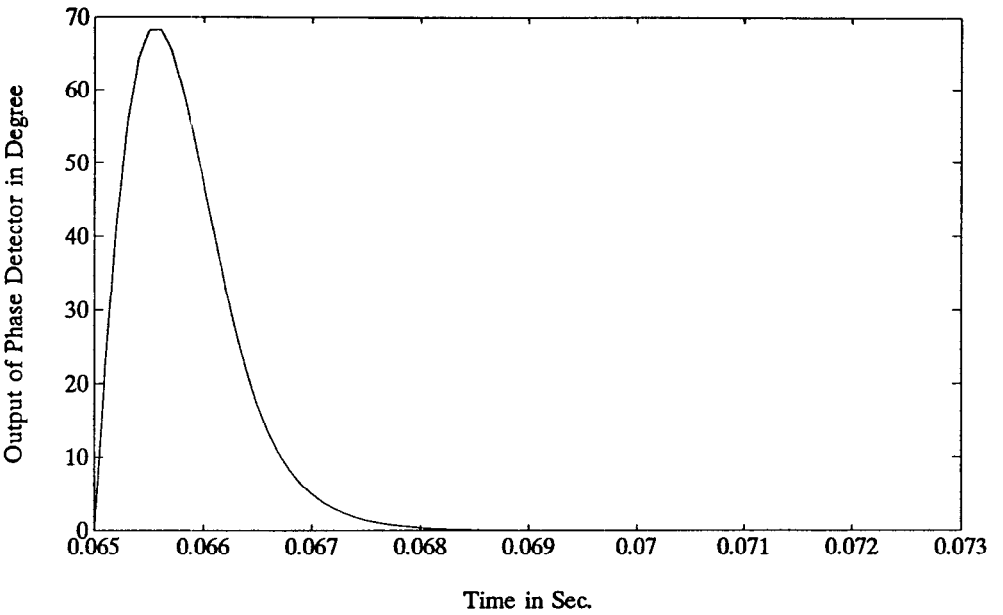

Fig.29. Output of the Phase Detector $\Delta\phi_1$ during Phase Pull-in.